Tension Monitoring and Defect Detection by Magnetostrictive Longitudinal Guided Wave for Fine Wire Rope

Wei Gao, Donglai Zhang, *Senior Member, IEEE*, and Xueli Zhu

***Abstract*— Fine wire rope is a type of skeleton material that is used widely in elevator steel belts, conveyor belts, and synchronous belts. When the tension of a fine wire rope changes abnormally, its service life and the safe operation of the system it belongs to will be seriously affected. Therefore, it is particularly important to monitor the tension and detect the defects of fine wire rope. However, traditional nondestructive testing technology only detects the defects or monitors the tension of the tested structure. In this article, longitudinal guided wave sensors are used to measure the tension changes and defects of fine wire rope. When the tension of a fine wire rope changes, the natural frequencies of the fine wire rope change, so the change of natural frequencies of fine wire rope can be used to represent the change of tension. White noise is used to measure the natural frequencies of fine wire rope under varying tension using a low-power circuit to determine the influence of the change of fine wire rope tension on the natural frequencies. Meanwhile, the excitation frequency needed to produce the maximum amplitude of the guided wave is determined according to the natural frequencies detection results to improve the signal-to-noise ratio of the guided wave signal. Additionally, defect detection is realized by analyzing the wave velocity and time of flight of the guided wave signal.**

***Index Terms*— Fine wire rope, magnetostrictive guided wave, natural frequencies, nondestructive testing, white noise.**

I. Introduction

Fine wire rope is a type of skeleton material that is applied widely in elevator steel belts, conveyor belts, and synchronous belts because it has a small diameter, high twist quality, high strand performance, and strong adhesion to surface materials. When the tension of a fine wire rope changes abnormally, its service life and the safe operation of the system it belongs to will be seriously affected. Therefore, it is particularly important to realize the tension monitoring and defect detection of fine wire rope. However, traditional nondestructive testing technology only detects the defects of the tested structure, so nondestructive testing technologies specifically designed for fine wire rope are needed. The nondestructive magnetic flux leakage testing technique is commonly used in the nondestructive testing of steel wire rope. Detection of magnetic flux leakage from steel wire rope not only allows the locations and sizes of defects to be detected but also enables the detection of internal defects in steel wire rope [1], [2]. In addition, online detection of wire ropes in complex electromagnetic environments can be realized through appropriate signal processing [3].

The magnetostrictive longitudinal guided wave method can detect defects in long pipes rapidly using single-point excitation with easy installation and no coupling requirements. This method is thus suitable for use in long-range nondestructive testing and structural health monitoring applications [4], [5]. To optimize the guided wave sensor for fine wire rope, a solution has been proposed in which three groups of permanent magnets are used to realize a static magnetic field, and a magnetoconductive device is conformed to the wire rope's surface. Three parallel clusters of solenoid coils are used in the excitation sensor, and three series clusters of solenoid coils are used in the detection sensor. This setup can increase the guided wave signal amplitude during wire rope testing [6]. The outer layer of the aluminum conductor steel-reinforced (ACSR) cable has no magnetostrictive effect, and the inner core has a weak magnetostrictive effect due to the aluminum strand, so the guided wave signal in the ACSR cable is weak. Additionally, the ACSR cable's surface is irregular, which means that it is difficult for a magnetostrictive sheet to adhere to this surface. Therefore, one study has proposed spraying an $Fe_{83}Ga_{17}$ powder coating onto the ACSR cable to generate the longitudinal wave required for defect detection [7]. In another study, it is shown that a piezoelectric guided wave sensor and a magnetostrictive guided wave sensor can realize defect detection in elevator wire ropes [8].

A combination of magnetic flux leakage testing and magnetostrictive guided wave testing has been used to detect defects at the fixed end and the free end of steel cables [9]. The relationship between the stress, the group velocity, and the phase velocity is determined through analysis of the stress characteristics of the steel wire rope to detect defects near the wire rope anchorage [10]. Electromagnetic acoustic transducer (EMAT) performance can be optimized through the transformer model [11]. The development of circuits for the excitation and reception of ultrasonic transducers allows fouling to be identified by the amplitude reduction of the received signal of guided waves [12].

Manuscript received September 1, 2020; revised December 24, 2020; accepted January 6, 2021. Date of publication January 22, 2021; date of current version February 2, 2021. This work was supported in part by the National Defense Basic Research Project under Grant JCKY20170603C017 and in part by the Shenzhen Municipal Commission of Science and Technology Innovation Project under Grant JCYJ20170413112018620. The Associate Editor coordinating the review process was Kamel Haddadi. *(Corresponding author: Donglai Zhang.)*

The authors are with the Power Electronic and Motion Control Research Center, Harbin Institute of Technology (Shenzhen), Shenzhen 518055, China (e-mail: gaowei6713@163.com; zhangdonglai@hit.edu.cn; 13713956812@163.com).

Digital Object Identifier 10.1109/TIM.2021.3052004

The tension of a wire rope affects its structure and the safety of the system it belongs to. The tension of wire rope is mainly analyzed according to the time–frequency characteristics of its guided wave. When using a guided wave to detect a steel wire rope, tension on the rope can cause a missing frequency band in the longitudinal guided wave, which is known as the notch frequency [13]. The notch frequency changes with the tension of the wire rope. Therefore, the relationship between the guided wave notch frequency and tension can be used as a new tension measurement method for wire rope [14]. When the tension of the wire rope is varied, the optimal excitation frequency of wire and wave velocity will also change [15], [16]. Additionally, the change in the tensile force will also cause the guided wave energy coupling between steel wires to change [17]. The amplitude of the harmonic generated by the application of an ultrasonic guided wave will change when the tension of the fine wire rope is varied [18].

Multifrequency excitation is used to improve the signal-to-noise ratio (SNR) of guided waves, and the detected signal contains rich frequency information that can be used in defect detection [19]. The natural frequencies of pipes can be determined via white noise excitation for magnetostrictive guided wave testing applications to increase the SNR of guided waves [20]. To enhance both the detection effect and the application range of magnetostrictive guided waves, several researchers have used magnetostrictive patch transducers, which can control the guided wave mode well and also improve the guided wave excitation efficiency. A good summary of magnetostrictive patch transducer technology is provided in [21].

To determine the tension and integrity of a fine wire rope, this article first uses white noise to determine the natural frequencies of the rope. The change of tension is judged by the change of natural frequencies of the rope. Then, the excitation frequency for the maximum amplitude of the guided wave is selected according to the natural frequencies to enhance the SNR of the guided wave. Finally, the defects in the fine wire rope are detected using magnetostrictive longitudinal guided waves. The rest of this article is arranged as follows. In Section II, the principles of magnetostrictive guided waves and white noise are presented. In Section III, experimental verification of the white noise-based measurements of the natural frequencies of fine wire rope is provided. The guided wave experimental verification procedure and its results are discussed in Section IV. In Section V, conclusions are presented.

II. Principle of Magnetostrictive Guided Wave

A. Principle of Magnetostrictive Guided Wave

Magnetostrictive guided wave detection is based on the principle of using both the positive effect and the inverse effect of these waves. Magnetostrictive guided wave detection involves the coupling of the electric, magnetic, and mechanical properties of the material under test. The expression for this coupling is

$$\varepsilon = E^H\sigma + dH \tag{1}$$

$$B = d^*\sigma + \mu H \tag{2}$$

where

- ε strain;
- E^{H} Young's modulus under a specific magnetic field;
- σ stress;
- d piezomagnetic coefficient;
- H magnetic field intensity;
- B magnetic induction intensity;
- d^* inverse piezomagnetic coefficient;
- μ permeability.

It is shown by the expression above that a change in the magnetic field will lead to elastic strain in ferromagnetic materials. Therefore, a change of this type can generate guided waves in ferromagnetic materials. When a guided wave produces an elastic strain in a ferromagnetic material, the magnetic field will change. Coupling between the mechanical field and the magnetic field can thus be realized.

When the guided wave signal is transformed from an electromagnetic signal into a mechanical vibration in the rope, the general elastic dynamic equations of motion (Navier–Stokes equations) for an isotropic elastic solid medium are as follows:

$$(\lambda + \mu_*)\nabla(\nabla \cdot u) + \mu_*\nabla^2 u = \rho\frac{\partial^2 u}{\partial t^2} \tag{3}$$

where

- u time resonance displacement vector;
- λ Lamé first constant;
- μ_* Lamé second constant;
- ρ material density.
- u is expressed using the Helmholtz decomposition

$$u = \nabla\phi + \nabla \times \varphi \tag{4}$$

$$\nabla \cdot \varphi = 0 \tag{5}$$

where

- φ dispersion vector;
- ϕ scalar potential.

By combining (3)–(5), the displacement component of the guided wave at any point in the rope in cylindrical coordinates is given by

$$\begin{cases} u_r = \dfrac{\partial\phi}{\partial r} + \dfrac{1}{r}\dfrac{\partial\varphi_z}{\partial\theta} - \dfrac{\partial\varphi_\theta}{\partial z} \\ u_\theta = \dfrac{1}{r}\dfrac{\partial\phi}{\partial\theta} + \dfrac{\partial\varphi_r}{\partial\theta} - \dfrac{\partial\varphi_z}{\partial r} \\ u_z = \dfrac{\partial\phi}{\partial z} + \dfrac{1}{r}\dfrac{\partial(r\varphi_r)}{\partial r} - \dfrac{1}{r}\dfrac{\partial\varphi_r}{\partial\theta}. \end{cases} \tag{6}$$

When a longitudinal wave is used to detect the ropes, the displacement field in the rope is given by

$$u_r \neq 0, \quad u_\theta = 0, \quad u_z \neq 0. \tag{7}$$

Equation (7) indicates that the longitudinal guided wave includes both radial and axial displacement. Therefore, the longitudinal wave is highly sensitive to circumferential defects and has a long propagation distance. The longitudinal wave can detect the internal and external defects of ropes, but it will also be affected by the media inside and outside these ropes. However, it is not sensitive to axial defects.

When a torsional wave is used to detect the defects in ropes, the displacement field in the rope is given as follows:

$$u_r = 0, \quad u_\theta \neq 0, \quad u_z = 0. \tag{8}$$

Equation (8) shows that the torsional wave only includes circumferential displacement. The torsional wave is thus sensitive to both circumferential and axial defects. It can also detect the internal and external defects of the ropes without being affected by the media inside and outside the ropes, but the transmission distance of this wave is short.

When a flexural wave is used to detect the defects in ropes, the displacement field in the ropes is given as follows:

$$u_r \neq 0, \quad u_\theta \neq 0, \quad u_z \neq 0. \tag{9}$$

Because the displacement of each component is not zero, axial, circumferential, and oblique defects can be detected using the flexural wave. However, flexural wave detection is rarely used in actual detection because it is easy to disperse this wave and generate other guided wave modes, which makes the signal detection process complex. Moreover, when the other two guided wave detection modes are used, the flexural wave will be suppressed as far as possible.

B. Principle of White Noise

Because a magnetostrictive sensor contains both static and dynamic magnetic fields, the magnetostrictive strain generated in the ropes is generally proportional to the excitation current

$$i(t) \propto \varepsilon(t). \tag{10}$$

It is assumed here that the magnetostrictive guided wave system is a linear system, which means that the transformation relationship among the frequency response function, the excitation, and the response is given by

$$H(j\omega) = \frac{w(j\omega)}{I(j\omega)} \tag{11}$$

where

$H(j\omega)$ Fourier transform of the system's frequency response;
$w(j\omega)$ Fourier transform of the response signal;
$I(j\omega)$ Fourier transform of the excitation signal $i(t)$.

When the excitation signal $i(t)$ is a white noise signal, $I(j\omega)$ represents a signal that has the same spectral energy density over the whole frequency domain, i.e., $I(j\omega)$ is a constant. When this signal is loaded into the magnetostrictive guided wave system, $w(j\omega)$ is the product of $H(j\omega)$ and a constant. Under the influence of the system's natural frequencies, the peak values of the spectrum in $w(j\omega)$ are the natural frequencies of the system. When a sine wave is used as the excitation signal, $I(j\omega)$ is the Fourier transform of the sine wave signal. Using the frequency response $H(j\omega)$, the detection signal of the system can then be obtained.

After the white noise signal is loaded into the longitudinal guided wave sensor, the natural frequencies of the rope can be obtained based on the system frequency response given in (11). However, because the energy of the white noise signal is low, the signal needs to be loaded into the rope for a specific period of time. The natural rope vibration characteristics then cause the vibration energy to accumulate gradually at the natural frequency points, while the vibration energy at nonnatural frequency points declines rapidly. Therefore, with the following steps, the natural frequencies of a rope can be obtained by analyzing the system's frequency response after it is loaded with white noise for a period of time.

1) The white noise signal is loaded into the magnetostrictive longitudinal wave sensor through a power amplifier.
2) The magnetostrictive guided wave sensor is used to record the system's data for a specified period of time. The data are then transmitted to a personal computer (PC).

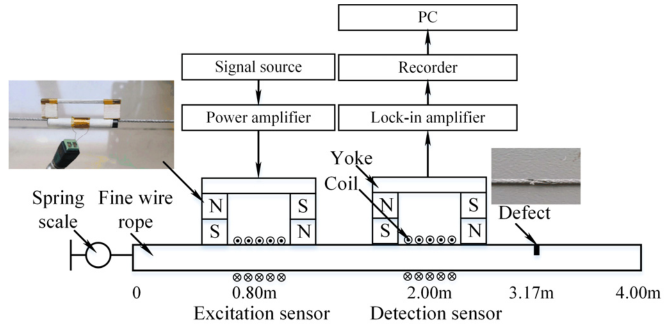

Fig. 1. Experimental diagram of fine wire rope.

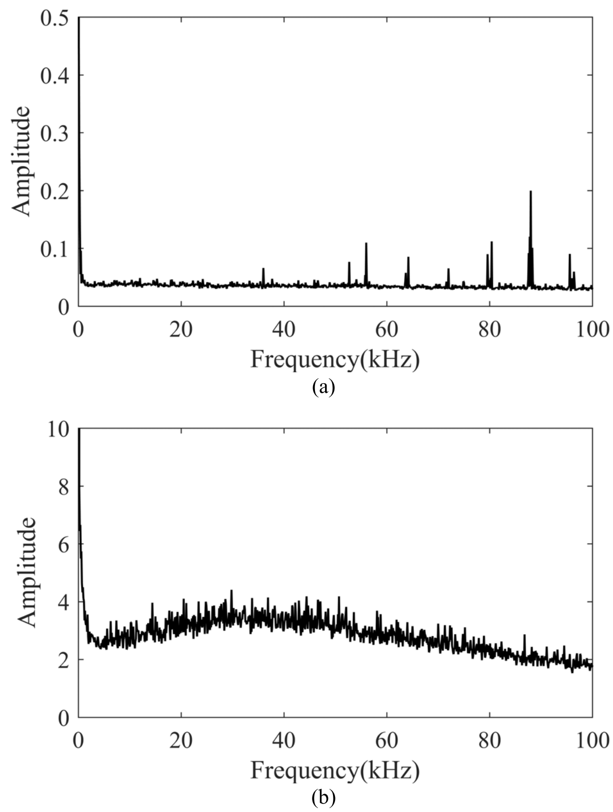

Fig. 2. (a) Spectrum envelopes of the detected signal without excitation signal. (b) Spectrum envelopes of excitation signal.

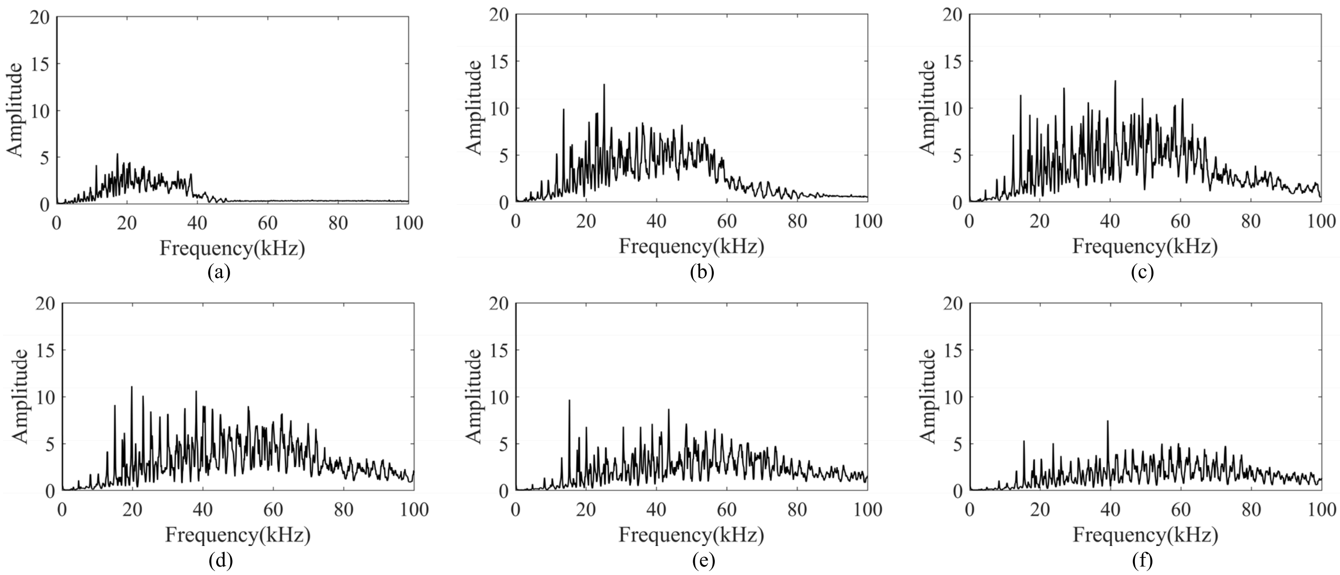

Fig. 3. Natural frequencies results for wire rope under different tensions. (a) 10-kg tension. (b) 20-kg tension. (c) 30-kg tension. (d) 40-kg tension. (e) 50-kg tension. (f) 60-kg tension.

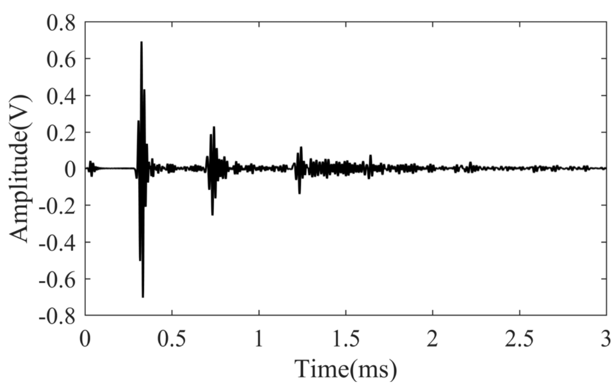

Fig. 4. 60-kHz guided wave signal of a wire rope without defects measured when the tension was 40 kg.

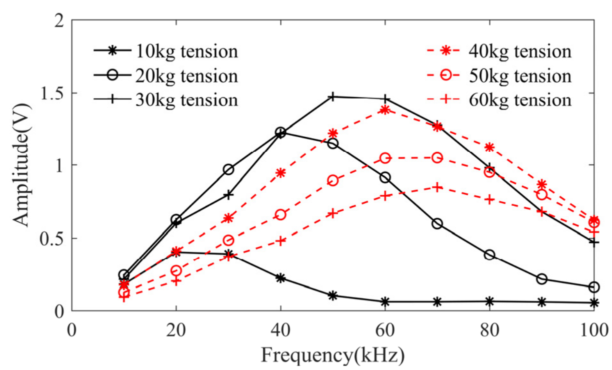

Fig. 5. Comparison of longitudinal guided wave amplitude results for the fine wire rope at different frequencies.

3) The PC is subsequently used to analyze the frequency characteristics of the measured data. The points in the spectrum with higher energy are the natural frequencies of the rope.

III. Experimental Verification of Natural Frequencies for Fine Wire Rope

An experiment is designed to verify the change in the natural frequencies of a wire rope under different tensions (Fig. 1). The diameter, length, and material of the wire rope are 2 mm, 4 mm, and Q235B, respectively. The length, width, and height of the sensor's yoke are 50, 2, and 2 mm, respectively. The yoke material is Q235B. The length, width, and height of the permanent magnet are 10, 2, and 10 mm, respectively. The magnetic field of this magnet is 280 kA/m. The magnetic material is NdFe35. The diameter of the wire coil is 0.2 mm, and the number of coils is 30. Two sensors are used to detect the fine wire rope. The excitation sensor is located 0.8 m away from the end of the rope, and the detection sensor is situated 1.2 m away from the excitation sensor. The defect is six broken wires.

The white noise signal is used to detect the natural frequencies of the fine wire rope under varying tension. The experimental steps of tension monitoring and guided wave defect detection for fine wire rope are as follows.

1) The white noise signal is loaded into the excitation sensor via the power amplifier.
2) The signal at the detection sensor is recorded for 10 s, and the detected signal is uploaded to the PC for fast Fourier transform (FFT) processing.
3) The natural frequencies of the wire rope are determined by analyzing the detected signal spectrum.
4) The change of tension is monitored by the change of natural frequencies of the wire rope. The excitation frequency of the guided wave with maximum amplitude is selected according to the natural frequencies.
5) The excitation frequency selected in step (4) is used to generate a guided wave to detect defects.

The results in Fig. 2(a) show the spectrum envelope of the detected signal with no excitation signal. Its spectrum remains constant in the low frequency band, and several energy peaks occur at higher frequencies. The maximum amplitude

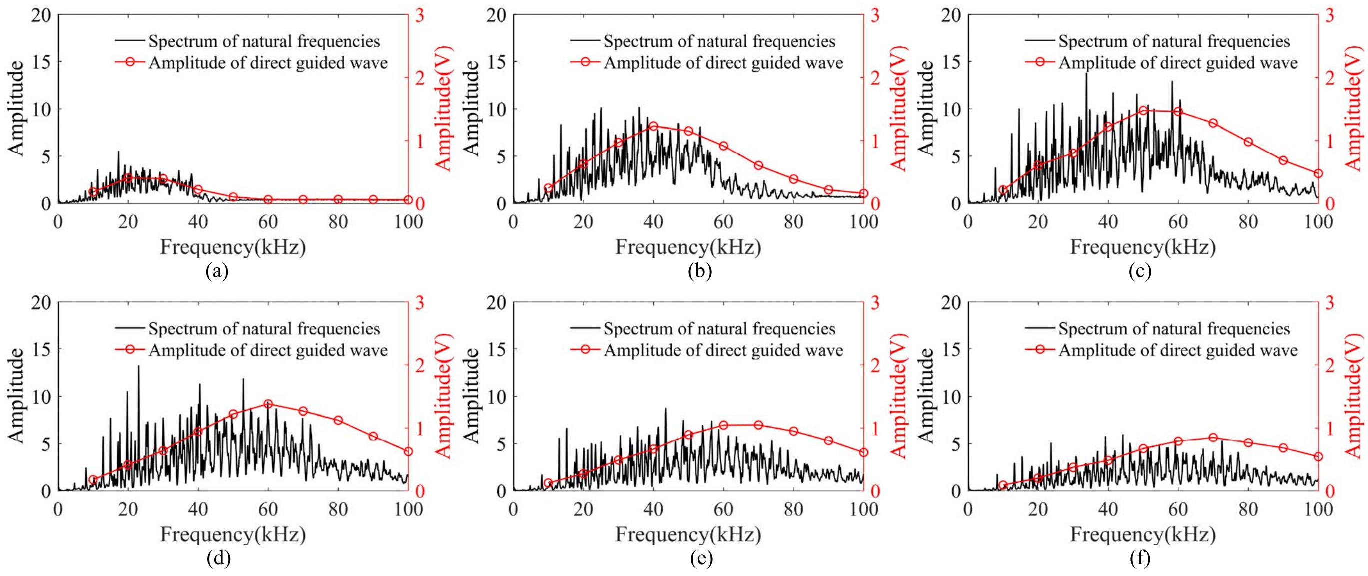

Fig. 6. Natural frequencies spectra and guided wave amplitudes of wire rope at different frequencies under various tensions. (a) 10-kg tension. (b) 20-kg tension. (c) 30-kg tension. (d) 40-kg tension. (e) 50-kg tension. (f) 60-kg tension.

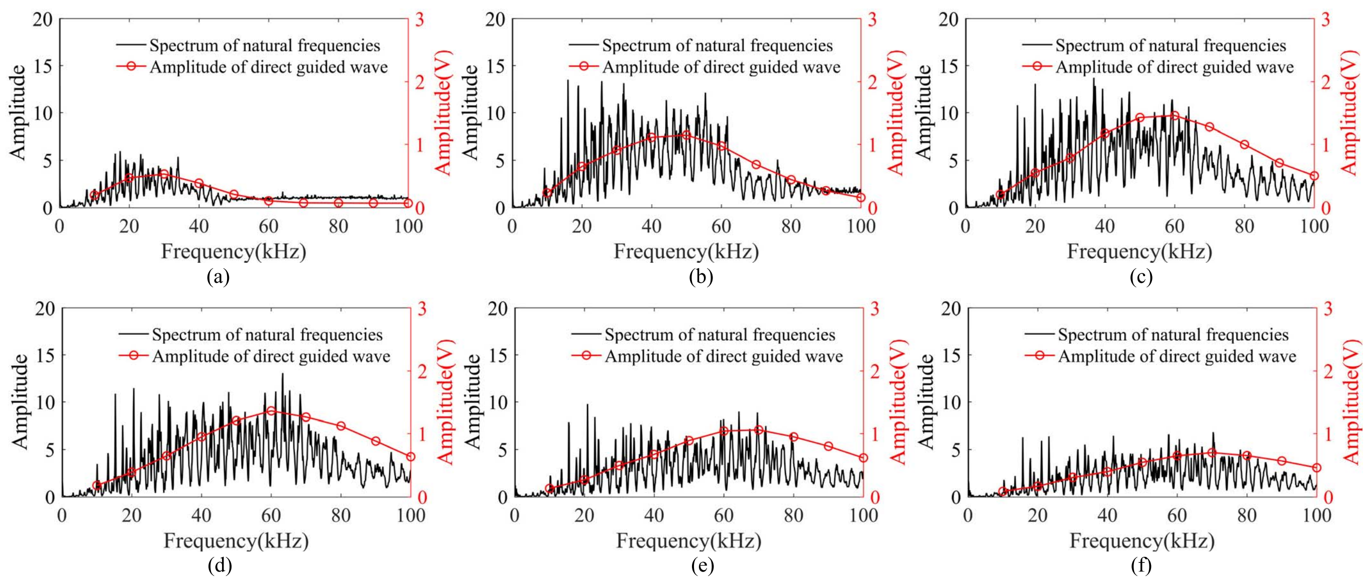

Fig. 7. Natural frequencies spectra and guided wave amplitudes of wire rope with defects at different frequencies under various tensions. (a) 10-kg tension. (b) 20-kg tension. (c) 30-kg tension. (d) 40-kg tension. (e) 50-kg tension. (f) 60-kg tension.

of the spectrum is approximately 0.2. This proves that the data acquisition system will not affect the detection of the natural frequencies of the fine wire rope. Fig. 2(b) shows the spectrum envelopes of the excitation signal. The spectral energy distribution of the excitation signal is uniform, and there is no obvious peak signal. Additionally, the energy of the spectrum decreases with increasing frequency.

When no defects are present in the wire rope, the natural frequencies under different tensions detected using white noise are as shown in Fig. 3. It can be seen from Fig. 3 that the natural frequencies of the wire rope increase gradually with increasing tension. At the same time, the energy density initially increases and then decreases with increasing frequency. The spectral energy density of the detected signal decreases with increasing tension when the tension is higher than 50 kg. Therefore, as the energy density of the white noise detection signal decreases, the guided wave amplitude also becomes smaller.

IV. Experimental Verification of Guided Waves Detection

To verify the relationship between the amplitude and the natural frequencies of the guided wave under different applied tensions, the sensor shown in Fig. 1 is used to realize excitation and detection of the longitudinal guided wave. The sensor parameters are similar to those used for white noise excitation.

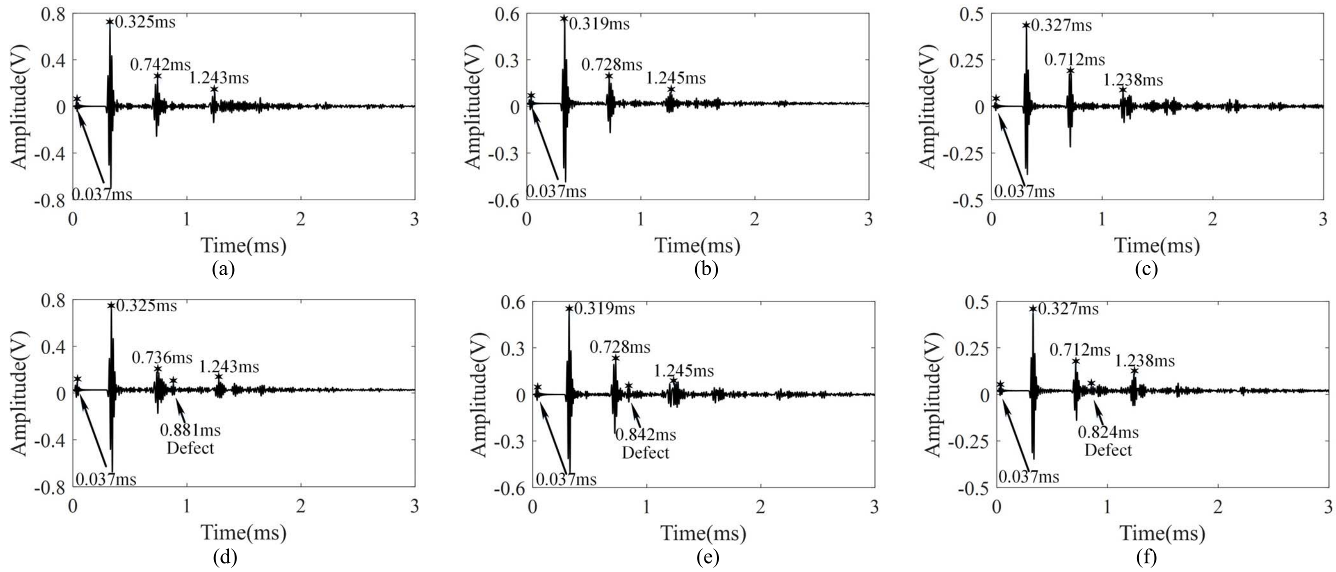

Fig. 8. 60-kHz longitudinal guided wave signals of fine wire ropes under various tensions. (a) Fine wire rope without defects at 40-kg tension. (b) Fine wire rope without defects at 50-kg tension. (c) Fine wire rope without defects at 60-kg tension. (d) Fine wire rope with defect at 40-kg tension. (e) Fine wire rope with defect 50-kg tension. (f) Fine wire rope with defect 60-kg tension.

The excitation waveform is a tone burst waveform that has two sine wave cycles with different frequencies. The burst period is 500 ms. When there are no defects in the wire rope, 40 kg of tension is applied to the wire rope. When the guided wave excitation frequency is 60 kHz, the guided wave signal is as shown in Fig. 4, which indicates that longitudinal guided waves can be generated using the sensor, but with some dispersion. The peak-to-peak value of the direct guided wave is approximately 1.38 V.

Comparison results for the guided wave amplitudes in the fine wire rope at different frequencies are shown in Fig. 5. The results show that when the wire rope tension is 30 kg and the excitation frequency is in the 0–100-kHz range, the direct guided wave amplitude initially increases and then decreases. The maximum amplitude occurs at the guided wave frequency of 20 kHz. When the wire rope tension is increased to 60 kg, the guided wave amplitude increases compared to the guided wave amplitude observed under 30-kg tension. The maximum amplitude occurs at a guided wave frequency of 70 kHz.

The white noise signal detection spectrum and direct guided wave amplitude results measured under different tensions are shown in Fig. 6. These results show that the white noise signal can reflect the variation in the guided wave amplitude accurately. When the spectral energy of the white noise detection signal is high, the peak-to-peak value of the guided wave will also be high. Therefore, the changes in the direct guided wave amplitude that occur at different frequencies can be verified using the white noise detection signal.

The guided wave excitation signal is a tone burst signal that contains two sine wave periods, and the pulse period is 500 ms. The spectral energy distribution of the excitation signal is relatively scattered, which means that the spectral energy distributions of the guided wave peak value and the white noise detection signal show some differences. When the number of periods of the excitation signal is increased, the spectral energy of the guided wave signal will gradually become concentrated, but the guided wave signals will overlap each other, so it will be difficult to distinguish the peak value of the guided wave signal.

When six broken wires are present in the wire rope, the experimental parameters are similar to the parameters of a wire rope without defects. The sensor parameters are similar to those used for white noise excitation. The excitation waveform is a tone burst waveform that has two sine wave cycles with different frequencies. The burst period is 500 ms. The test results for the natural frequencies of the wire rope under different tensions are shown in Fig. 7. These results show that the natural frequencies of the wire rope increase gradually with increasing tension. Simultaneously, the energy density initially increases and then decreases with increasing frequency. The law for this wire rope is similar to that for the wire rope without defects.

The 60-kHz guided wave signal recorded when the tension is 40 kg is shown in Fig. 8. Based on the guided wave signal shown in Fig. 8, the velocity of the guided wave is given by

$$v = \frac{1.2 \text{ m}}{0.325 \text{ ms} - 0.037 \text{ ms}} = 4.17 \text{ m/ms} \tag{12}$$

where 1.2 m is the distance between the excitation sensor and detection sensor, 0.037 ms is the time of the excitation signal, and 0.325 ms is the time when the direct guided wave reaches the detection sensor.

In Fig. 8(d), the time of flight of the defect guided wave signal is 0.881 ms. The velocity of the guided wave is 4.17 m/ms, so the propagation distance of the defect guided wave is 3.67 m. Since the distance between the defect and the detection sensor is 1.17 m, the defect guided wave should be transmitted 3.54 m. Therefore, the position of the defect error is 3.67%. Comparison results for the 60-kHz guided wave signal for wire ropes with and without a defect under loads

TABLE I
RESULTS OF DEFECT GUIDED WAVE

Tension	Velocity of the guided wave	Time of flight for the defect guided wave	Position of defect error
40 kg	4.17 m/ms	0.881 ms	3.67 %
50 kg	4.26 m/ms	0.843 ms	3.11%
60 kg	4.14 m/ms	0.824 ms	7.96 %

of 40, 50, and 60 kg are shown in Fig. 8. The law for this wire rope is similar to that for the wire rope without defects. The calculation procedures of guided wave signal for the fine wire ropes under loads of 50 and 60 kg are similar to that for the fine wire rope under a load of 40 kg. The results of the defect guided wave are shown in Table I, including the guided wave velocity and the time of flight of the guided wave signal.

The results in Table I show that the defect is detected and its position is obtained using the guided wave signal. Because of the spiral structure of the fine wire rope, the guided wave can easily become dispersed and distorted. At the same time, the attenuation rate of the guided wave increases with increasing frequency. When defects are present, guided waves will suffer from mode conversion and other problems, which will increase the signal complexity.

A wire rope is made using several wires in spiral shapes, and there are gaps between these wires. Because of the influence of the eddy current effect, the dynamic magnetic distribution from the surface toward the center of the wire rope decreases gradually. Therefore, the outer layer of the wire rope produces the strongest guided wave. When the tension in the wire rope increases, the contact between the wires in the wire rope becomes closer. Therefore, more of the energy of the outer guided wave propagates toward the interior, which causes the tension of the wire rope to increase and the amplitude of the guided wave to decrease.

V. CONCLUSION

In this article, longitudinal guided wave sensors are used to measure the tension changes and defects of fine wire rope. White noise is used to measure the natural frequencies of fine wire rope under different tensions using a low-power circuit to determine the influence of the change of fine wire rope tension on the natural frequencies. Meanwhile, the excitation frequency needed to produce the maximum amplitude of the guided wave is determined according to the natural frequencies detection results to improve the SNR of the guided wave signal. Additionally, defect detection is realized by analyzing the wave velocity and time of flight of the guided wave signal. From the experimental results, it is found that when the tension in the fine wire rope increases, its natural frequencies will increase. The energy density of the wire rope will decrease with this increase in tension. The longitudinal guided wave verification method indicates that as the spectrum of the white noise detection signal increases, the direct guided wave amplitude also increases. The measurement method can reflect the variation of the guided wave amplitude using the white noise detection signal spectrum, which provides a specific basis for the longitudinal guided waves being influenced by the wire rope tension.

REFERENCES

[1] D. L. Zhang, Y. N. Cao, C. Wang, and D. G. Xu, "A new method of defects identification for wire rope based on three-dimensional magnetic flux leakage," *J. Phys., Conf. Ser.*, vol. 48, pp. 334–338, Oct. 2006.

[2] Y. Cao, D. Zhang, C. Wang, and D. Xu, "More accurate localized wire rope testing based on Hall sensor array," *Mater. Eval.*, vol. 64, no. 9, pp. 907–910, Sep. 2006.

[3] X. Yan, D. Zhang, S. Pan, E. Zhang, and W. Gao, "Online nondestructive testing for fine steel wire rope in electromagnetic interference environment," *NDT & E Int.*, vol. 92, pp. 75–81, Dec. 2017.

[4] H. Kwun and K. A. Bartels, "Magnetostrictive sensor technology and its applications," *Ultrasonics*, vol. 36, nos. 1–5, pp. 171–178, Feb. 1998.

[5] H. Kwun, S. Y. Kim, and G. M. Ligh, "The magnetostrictive sensor technology for long range guided wave testing and monitoring of structures," *Mater. Eval.*, vol. 61, no. 1, pp. 80–84, 2003.

[6] Z. Liu, J. Zhao, B. Wu, Y. Zhang, and C. He, "Configuration optimization of magnetostrictive transducers for longitudinal guided wave inspection in seven-wire steel strands," *NDT & E Int.*, vol. 43, no. 6, pp. 484–492, Sep. 2010.

[7] F. Lv, P. Zhang, Z. Tang, Y. Yue, and K. Yang, "A guided wave transducer with sprayed magnetostrictive powder coating for monitoring of aluminum conductor steel-reinforced cables," *Sensors*, vol. 19, no. 7, p. 1550, Mar. 2019.

[8] W. T. Peter and J. M. Chen, "Effective guided wave technique for performing non-destructive inspection on steel wire ropes that hoist elevators," presented at the 8th World Congr. Eng. Asset Manage., Hong Kong, China, 2013, pp. 309–320.

[9] J. Xu, X. Wu, C. Cheng, and A. Ben, "A magnetic flux leakage and magnetostrictive guided wave hybrid transducer for detecting bridge cables," *Sensors*, vol. 12, no. 1, pp. 518–533, Jan. 2012.

[10] F. L. di Scalea, P. Rizzo, and F. Seible, "Stress measurement and defect detection in steel strands by guided stress waves," *J. Mater. Civil Eng.*, vol. 15, no. 3, pp. 219–227, Jun. 2003.

[11] M. Seher and R. Challis, "The electrical properties of a planar coil electromagnetic acoustic transducer and their implications for noise performance," *Meas. Sci. Technol.*, vol. 27, no. 2, Feb. 2016, Art. no. 025102.

[12] J. J. da Silva, M. G. Wanzeller, P. de Almeida Farias, and J. S. da Rocha Neto, "Development of circuits for excitation and reception in ultrasonic transducers for generation of guided waves in hollow cylinders for fouling detection," *IEEE Trans. Instrum. Meas.*, vol. 57, no. 6, pp. 1149–1153, Jun. 2008.

[13] H. Kwun, K. A. Bartels, and J. J. Hanley, "Effects of tensile loading on the properties of elastic-wave propagation in a strand," *J. Acoust. Soc. Amer.*, vol. 103, no. 6, pp. 3370–3375, Jun. 1998.

[14] X. Liu, B. Wu, F. Qin, C. He, and Q. Han, "Observation of ultrasonic guided wave propagation behaviours in pre-stressed multi-wire structures," *Ultrasonics*, vol. 73, pp. 196–205, Jan. 2017.

[15] S. Chaki and G. Bourse, "Guided ultrasonic waves for non-destructive monitoring of the stress levels in prestressed steel strands," *Ultrasonics*, vol. 49, no. 2, pp. 162–171, Feb. 2009.

[16] A. Frikha, F. Treyssède, and P. Cartraud, "Effect of axial load on the propagation of elastic waves in helical beams," *Wave Motion*, vol. 48, no. 1, pp. 83–92, Jan. 2011.

[17] I. Bartoli, R. Phillips, F. L. di Scalea, S. Salamone, S. Coccia, and C. S. Sikorsky, "Load monitoring in multiwire strands by interwire ultrasonic measurements," *Proc. SPIE*, vol. 6932, Apr. 2008, Art. no. 693209.

[18] C. Nucera and F. L. di Scalea, "Monitoring load levels in multi-wire strands by nonlinear ultrasonic waves," *Struct. Health Monitor.*, vol. 10, no. 6, pp. 617–629, Nov. 2011.

[19] D. Zhang, Z. Zhou, J. Sun, E. Zhang, Y. Yang, and M. Zhao, "A magnetostrictive guided-wave nondestructive testing method with multifrequency excitation pulse signal," *IEEE Trans. Instrum. Meas.*, vol. 63, no. 12, pp. 3058–3066, Dec. 2014.

[20] D. Zhang, W. Gao, and X. Yan, "Determination of natural frequencies of pipes using white noise for magnetostrictive longitudinal guided-wave nondestructive testing," *IEEE Trans. Instrum. Meas.*, vol. 69, no. 6, pp. 2678–2685, Jun. 2020.

[21] Y. Y. Kim and Y. E. Kwon, "Review of magnetostrictive patch transducers and applications in ultrasonic nondestructive testing of waveguides," *Ultrasonics*, vol. 62, pp. 3–19, Sep. 2015.